Journal of Engineering Physics and Thermophysics, Vol. 75, No. 4, 2002

NUMERICAL SIMULATION OF TURBULENT HEAT TRANSFER IN A ROTATING DISK AT ARBITRARY DISTRIBUTION OF THE WALL TEMPERATURE

I. V. Shevchuk

UDC 536.24

Turbulent heat transfer in a freely rotating disk with an arbitrary change in the wall temperature is investigated. With the aid of the integral method developed previously, numerical simulation for the cases of positive, approximately constant, and negative radial temperature gradients of the disk is carried out. Unlike the known Dorfman method, the results of the calculations performed agree well with experimental data. Based on the data obtained, conclusions are drawn about relatively optimum parameters of the model for the conditions under consideration.

Investigation of different aspects of turbulent heat transfer in a rotating disk is a topical problem as applied to the systems of air cooling of the rotors of gas turbines, hard disks of computers, etc. It is well known that an analytical solution of the problem [1–5] obtained by the integral method with power-law radial distribution of the disk temperature is as follows:

$$T_{\mathrm{w}} - T_{\infty} = c_0 r^{n_*}, \tag{1}$$

$$\mathrm{Nu} = K_1 \, \mathrm{Re}_{\varphi}^{n_R} x^{m_x}, \tag{2}$$

where $n_R = (n + 1)/(3n + 1)$, K_1, c_0, and n_* are constants. The quantity n is an exponent of the power approximation of the velocity and temperature profiles. The constant m_x in formula (2) acquires a value of $m_x = 1 + m$ at condition (1). In the case of turbulent flow, $n = 1/5$–$1/10$ and $m = (1 - n)/(3n + 1)$; in the case of laminar flow, $n = 1$ and $m = 0$. At an arbitrary value of m_x, in [6] a more general analytical solution is obtained for the wall temperature T_{w} that includes relation (1) as a particular case. Analysis has shown that the solution of the problem obtained by the author of [4–6] is the most exact one, while in a number of cases the calculations by the Dorfman formula [1–3] substantially exceed the reliable experimental and calculated data obtained by other authors.

However, under real conditions often the wall temperature distribution cannot be described by the analytical dependences mentioned above. In these cases, use is made of a numerical version of the integral method and the distribution of T_{w} is approximated by some other dependence. In [7, 8], the Dorfman method at a fixed value of $n = 1/7$ was employed for numerical simulation of the conditions observed in experiments. As in the case of the analytical version of the Dorfman method, the calculated results for a Nusselt number [7, 8] markedly exceeded the experimental data at $dT_{\mathrm{w}}/dr \approx 0$ and $dT_{\mathrm{w}}/dr < 0$. The calculated and experimental results agreed well at $dT_{\mathrm{w}}/dr > 0$, with the exception of the cases of high Re_{φ} numbers at which the calculated data were lower than the experimental values.

The authors of [9] simulated the experimental conditions of [7, 8] by solving numerically the differential equations for a boundary layer with use of the known Cebeci–Smith model of turbulent viscosity [10]. The agreement of the calculations with the experiments turned to be good. This is indicative of the reliability of the experimental data of [7, 8], while the substantial error of the Dorfman method at $dT_{\mathrm{w}}/dr \le 0$ is responsible for the disagreement of the calculated [7, 8] and experimental results.

Institute of Engineering Thermal Physics, National Academy of Sciences of Ukraine, Kiev; email: ivshevch@i.com.ua. Translated from Inzhenerno-Fizicheskii Zhurnal, Vol. 75, No. 4, pp. 94–97, July–August, 2002. Original article submitted March 28, 2001.

1062-0125/02/7504-0885$27.00

In the present work, with the aid of the integral method [3, 4, 11, 12] numerical simulation of the turbulent heat transfer in a rotating disk is carried out under experimental conditions [7, 8]. Consideration is given to the cases of positive, approximately constant, and negative values of dT_w/dr.

Integral Method. Integral equations for dynamic and thermal boundary layers are of the form

$$\frac{d}{dr}\left[\delta r\int_0^r v_r^2 d\xi\right]-\delta\int_0^1 v_\varphi^2 d\xi=-r\tau_{wr}/\rho\,, \tag{3}$$

$$\frac{d}{dr}\left[\delta r^2\int_0^1 v_r v_\varphi d\xi\right]=-r^2\tau_{w\varphi}/\rho\,, \tag{4}$$

$$\frac{d}{dr}\left[\delta_T r\int_0^1 v_r\,(T-T_\infty)\,d\xi_T\right]=rq_w/(\rho c_p)\,. \tag{5}$$

The velocity profiles v_φ and v_r, the shear stresses $\tau_{w\varphi}$ and τ_{wr}, the temperature profile T, and the local numbers Nu are determined by the following expressions [4, 5]:

$$\bar{v}_\varphi=\xi^n\,,\quad \bar{v}_r=\bar{v}_\varphi\alpha\,(1-\xi)^2\,; \tag{6}$$

$$\tau_{wr}=-\alpha\tau_{w\varphi}\,,\quad \tau_{w\varphi}=-\tau_w\,(1+\alpha^2)^{-1/2}\,; \tag{7}$$

$$c_f/2=\tau_w/(\rho V_*)^2=C_n^{-2/(n+1)}\,\mathrm{Re}_{V_*}^{-2n/(n+1)}\,; \tag{8}$$

$$(T-T_w)/(T_\infty-T_w)=\xi_T^{n_T}\,; \tag{9}$$

$$\mathrm{Nu}=\mathrm{St}\,\frac{\rho V_* r}{\mu}\,\mathrm{Pr}\,; \tag{10}$$

$$\mathrm{St}=C_n^{(n_T-1)/(1-n)}\,\mathrm{Re}_{V_*}^{-n_T}\,(c_f/2)^{(1-n_T)/2}\,\Delta^{-n_T}\,\mathrm{Pr}^{-n_p}\,. \tag{11}$$

Here $\bar{v}_\varphi=(\omega r-v_\varphi)/\omega r$; $\bar{v}_r=v_r/(\omega r)$; $\mathrm{Re}_{V_*}=\rho V_*\delta/\mu$; $V_*=\omega r(1+\alpha^2)^{1/2}$; $C_n=2.28+0.924/n$. In the general case, the constant $n_T=1/5$–$1/10$ differs from n.

After integration with account for formulas (6)–(11) the equations for the boundary layer (3)–(5) are reduced to a form in which they are solved numerically by the Runge–Kutta method. In the equations α, δ, and Δ are the unknown quantities. The details of the procedure are described in [11, 12].

Local Heat Transfer. Comparison with Experiments. In the present work, for analysis use is made, as in [9], of the experimental temperatures of the disk corresponding to determination of the Nu number from the measurements with the aid of pickups of a local heat flux [7, 8]. The Nu numbers in such a way are corrected by subtracting the radiation component following the procedure in [8].

The experimental surface temperature distributions of the disk [7, 8] are subdivided by the authors into four groups and characterized as those conventionally obeying distribution (1) at $n_*=-0.2$, 0.1, 0.4, and 0.6. Examples of such distributions for a number of Re_φ values are given in Fig. 1. Inside each group the T_w distributions differed, as

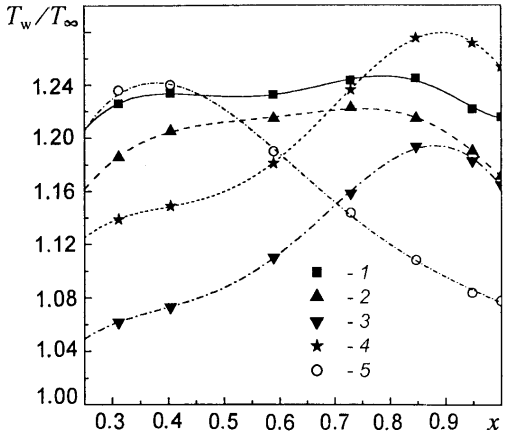

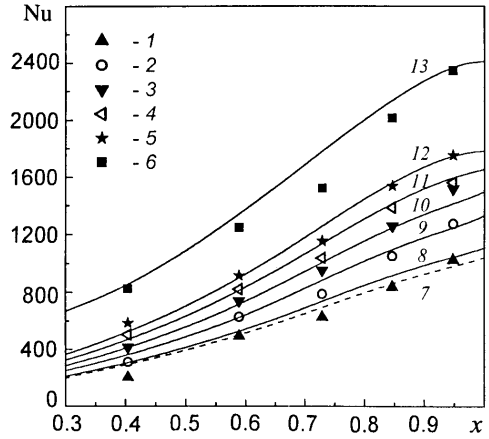

Fig. 1. Radial changes in the disk temperature T_w/T_∞ (points, experiments [7, 8], curves, their polynomial approximation): 1) conventionally $n_* = 0.1$, $Re_\varphi = 1.35\cdot10^6$; 2) 0.1 and $3.2\cdot10^6$; 3) 0.4 and $3.14\cdot10^6$; 4) 0.6 and $1.59\cdot10^6$; 5) –0.2 and $2.65\cdot10^6$.

Fig. 2. Radial change in the Nu number, conventionally $n_* = 0.1$; 1–6) experiments [7, 8]; 7) calculation at $n = 1/6$, $n_T = 1/5$; 8–13) calculation at $n = n_T = 1/6$; 1, 7, and 8), $Re_\varphi = 1.08\cdot10^6$; 2 and 9) $1.35\cdot10^6$; 3 and 10) $1.6\cdot10^6$; 4 and 11) $1.88\cdot10^6$; 5 and 12) $2.14\cdot10^6$; 6 and 13) $3.2\cdot10^6$.

a maximum, by 10–15% for different Re_φ, but at the same time they had approximately the same general trend of the curves (see, e.g., curves 1 and 2 for the case conventionally $n_* = 0.1$). These curves are characterized mainly by the positive ($n_* = 0.4$ and 0.6), approximately constant ($n_* = 0.1$), and negative ($n_* = -0.2$) gradients of the wall temperature.

The correspondence of dependence (1) to the experiments at the n_* indicated above is rather conventional. For instance, formula (1) has no extreme (either inflection) points inside the region of determination of T_w over the disk radius. At the same time, all the dependences depicted in Fig. 1 have the characteristic points. However, for the sake of convenience the conventional subdivision of the curves into groups adopted in [7, 8] is retained in the present work.

The discrete experimental values of the temperature disk (the tabular data of [8]) were approximated in the present work in the form of a polynomial of the seventh degree to be used in calculations by the integral method. Examples of such dependences are shown in Fig. 1.

The results of calculations of changes in the local Nu numbers are given in Figs. 2–4. Their common feature is the nonuniversality of the n and n_T values. However, a comparison of the calculated curves with the experimental ones makes it possible to draw some qualitative and quantitative conclusions about regularities of the choice of the n and n_T values for particular thermal and hydrodynamic conditions. It should be also noted that the calculated curves in these figures agree well with the calculations [9] carried out, as indicated above, by the differential method.

Results of simulation of the case $n_* = 0.1$ are presented in Fig. 2. The calculations have been carried out mainly at $n = n_T = 1/6$. Agreement of the calculated and experimental data is good, though at $Re_\varphi = 1.08\cdot10^6$ the values $n = 1/6$ and $n_T = 1/5$ at $x \le 0.85$ allow slightly better agreement. This can be apparently attributed to the trend toward decreasing n_T at sufficiently small Reynolds numbers Re_ω.

Figure 3 shows the results of simulation of the sufficiently similar cases $n_* = 0.4$ and $n_* = 0.6$. At lower values of $Re_\omega = (1.59–1.71)\cdot10^6$, good agreement with experiments can be attained by using $n = n_T = 1/6.5$. For higher values of $Re_\omega = (2.67–3.14)\cdot10^6$, it is necessary to use $n = n_T = 1/7$ or 1/6. It should be noted that for the data given in Fig. 3 n and n_T are, on the whole, slightly smaller as compared to the case $n_* = 0.1$ (Fig. 1). At Re_φ = idem, the only difference in the boundary conditions for the compared calculated data is the value of the radial temperature gradient of the disk. For Fig. 2, $dT_w/dr \approx 0$ while for Fig. 3, $dT_w/dr > 0$.

The assumption about the influence of dT_w/dr on the exponents n and n_T is confirmed by the calculated data in Fig. 4 for the case $n_* = -0.2$. For lower values of $Re_\varphi = (0.548–1.08)\cdot10^6$, one needed to choose $n_T = 1/4$ at $n =$

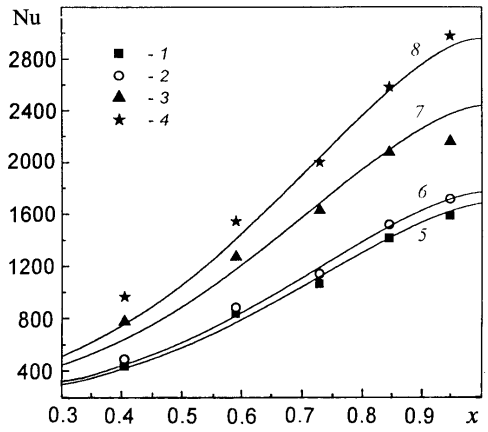

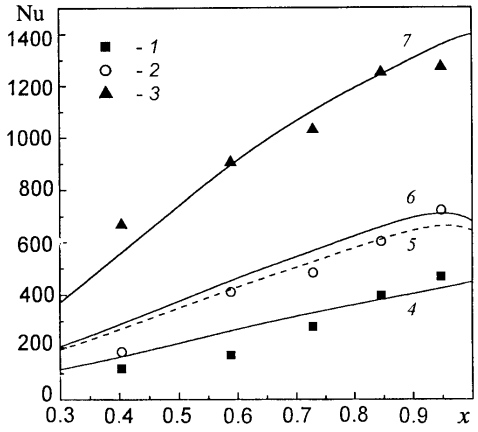

Fig. 3. Radial change in the Nu number, conventionally $n_* = 0.6$; 1 and 2) experiments [7, 8]; 5 and 6) calculation at $n = n_T = 1/6.5$; 1 and 5) $\mathrm{Re}_\varphi = 1.59 \cdot 10^6$; 2 and 6) $1.71 \cdot 10^6$; conventionally $n_* = 0.4$; 3 and 4) experiments [7, 8]; 7) calculation at $n = n_T = 1/6$; 8) calculation at $n = n_T = 1/7$; 3 and 7) $\mathrm{Re}_\varphi = 2.67 \cdot 10^6$; 4 and 8) $3.14 \cdot 10^6$.

Fig. 4. Radial changes in the Nu number, conventionally $n_* = -0.2$; 1, 2, and 3) experiments [7, 8]; 4 and 5) calculation at $n = 1/6$, $n_T = 1/4$; 6 and 7) calculation at $n = 1/6$, $n_T = 1/5$; 1 and 4) $\mathrm{Re}_\varphi = 0.548 \cdot 10^6$; 2, 5, and 6) $1.08 \cdot 10^6$; 3 and 7) $2.65 \cdot 10^6$.

1/6. At a higher value of $\mathrm{Re}_\varphi = 2.56 \cdot 10^6$, we have $n_T = 1/5$ (a lower value) at the same $n = 1/6$. Thus, the influence of $dT_\mathrm{w}/dr < 0$ is evident again as compared to Fig. 2: at Re_φ = idem the same $n = 1/6$ is retained and n_T increases.

The characteristic feature of the data in Figs. 2–4 is the dip of the experimental Nu numbers [7, 8] at the point $x \approx 0.73$ in relation to the calculations. The same disagreement of the experiments and calculations at $x \approx 0.73$ is noted also in [9]; apparently, the reason lies in the systematic error of experimental measurements [7, 8] at the point.

It should be noted that in the experiments [7, 8] the velocity and temperature profiles have not been measured; therefore, the above analysis of the exponents n and n_T is based on the Nu numbers obtained indirectly. Nevertheless, taking into consideration the interrelation between $n = n_T$ and the exponent n_R at the Reynolds number in formula (2) for Nu at condition (1), this analysis can be believed to be quite justified. Thus, at $n = n_T = 1/7$ we have $n_R = 0.8$, $m_x = 1.6$. It is evident that the rate of increasing the Nu numbers over the radius in Figs. 2 and 4 (the cases $n_* = 0.2$ and 0.1) corresponds to the smaller n_R and m_x and, consequently, to the larger n and n_T, which is confirmed by numerical calculations. Moreover, it is interesting to note that the authors of [13], experimentally measuring the temperature profiles at the negative value of dT_w/dr in the case q_w = const (or $n_* \approx -0.6$), have obtained $n_T = 1/4$–$1/5$ for $\mathrm{Re}_\omega = 10^6$. This agrees with the data of the present investigation for $n_* = -0.2$.

CONCLUSIONS

1. The results of numerical simulation of the turbulent heat transfer in a rotating disk with the aid of the developed integral method agrees well with the known experimental data [7, 8].

2. The calculations carried out allow us to assert that the boundary conditions of the problem exert an influence on the parameters of the model and to suggest the optimum values of these parameters for the conditions under consideration.

NOTATION

b, outer radius of the disk, m; c_p, heat capacity at constant pressure, J/(kg·K); $\mathrm{Nu} = q_\mathrm{w} r/[\lambda(T_\mathrm{w} - T_\infty]$, local Nusselt number; $\mathrm{Pr} = \mu c_p/\lambda$, Prandtl number; q_w, heat flux on the wall, W/m^2; r, φ, and z, radial, tangential, and axial coordinates; $\mathrm{Re}_\omega = \rho\omega r^2/\mu$, local rotational Reynolds number; $\mathrm{Re}_\omega = \rho\omega b^2/\mu$, rotational Reynolds number over

the outer radius; St = $q_w/[\rho V_* c_p(T_w - T_\infty)]$, Stanton number; T, temperature, K; v_r, v_φ, and v_z, radial, tangential, and axial velocities, m/sec; $x = r/b$, dimensionless radial coordinate; α, tangent of the torsion angle on the wall; δ and δ_T, thicknesses of the dynamic and thermal boundary layers, m; $\Delta = \delta_T/\delta$, relative thickness of the thermal boundary layer; λ, thermal conductivity, W/(m·K); μ, coefficient of dynamic viscosity, Pa·sec; $\xi = z/\delta$ and $\xi_T = z/\delta_T$, dimensionless normals to the coordinate surface; ρ, density, kg/m^3; $\tau_w = (\tau_{wr}^2 + \tau_{w\varphi}^2)^{1/2}$, total shear stress of friction on the wall, Pa; $\tau_{w\varphi} = \mu(\partial v_\varphi/dz)_{z=0}$ and $\tau_{wr} = \mu(\partial v_r/dz)_{z=0}$, tangential and radial shear stresses of friction on the wall, Pa; ω, angular speed of rotation, 1/sec. Subscripts: w, wall; ∞, external boundary of the boundary layer.

REFERENCES

1. L. A. Dorfman, *Drag and Heat Transfer of Rotating Bodies* [in Russian], Moscow (1960).
2. I. T. Shvets and E. P. Dyban, *Air Cooling of Parts of Gas Turbines* [in Russian], Kiev (1974).
3. J. M. Owen and R. H. Rogers, *Flow and Heat Transfer in Rotating-Disk Systems*, Vol. 2, *Rotating Cavities*, Taunton (Somerset), England (1995).
4. I. V. Shevchuk, *Prom. Teplotekh.*, **22**, No. 2, 25–30 (2000).
5. I. V. Shevchuk, *Teplofiz. Vys. Temp.*, **38**, No. 3, 521–523 (2000).
6. I. V. Shevchuk, *Prom. Teplotekh.*, **22**, Nos. 5–6, 5–9 (2000).
7. A. Northrop and J. M. Owen, *Int. J. Heat Fluid Flow*, **9**, No. 1, 27–36 (1988).
8. A. Northrop, *Heat Transfer in a Cylindrical Rotating Cavity*, D. Phil. Thesis, Univ. of Sussex, Brighton, UK (1984).
9. C. L. Ong and J. M. Owen, *Int. J. Heat Fluid Flow*, **12**, No. 2, 106–115 (1991).
10. T. Cebeci and A. M. O. Smith, *Analysis of Turbulent Boundary Layers*, New York (1974).
11. I. V. Shevchuk, *Prom. Teplotekh.*, **19**, No. 6, 18–23 (1997).
12. I. V. Shevchuk, *Prom. Teplotekh.*, **20**, No. 1, 54–58 (1998).
13. C. J. Elkins and J. K. Eaton, *Heat Transfer in the Rotating Disk Boundary Layer*, Stanford Univ., Dept. of Mech. Eng., Thermosci. Div., Rep. TSD-103 (1997).